Nanoscale

RSC Publishing

COMMUNICATION

View Article Online
View Journal | View Issue

Cite this: *Nanoscale*, 2013, **5**, 10835

Light extraction – a practical consideration for a plasmonic nano-ring laser

Chee-Wei Lee,* Gurpreet Singh and Qian Wang

Received 15th August 2013
Accepted 10th September 2013

DOI: 10.1039/c3nr04327d

www.rsc.org/nanoscale

An integrated semiconductor plasmonic nano-ring laser with a connecting output plasmonic waveguide for light extraction is proposed, designed and demonstrated numerically. The maximum light extraction efficiency can be up to 56%. The design was optimized with 2D FDTD and verified with 3D FDTD methods, where close agreement is shown between the two.

Semiconductor-plasmonic nanolasers have been of great interest over recent years due to their ultra-small footprint, very low power consumption and high modulation bandwidth, which make them promising as on-chip light sources for intra-chip data interconnects, high-density data storage, lab-on-chip applications, *etc*. Various plasmonic nanolaser structures have been reported either theoretically or experimentally in the published literature, and include bow-tie antennas, Fabry–Perot lasers, nano-patch lasers, nanodisks, coaxial and ring lasers.[1–11] However, most of the reported works, apart from just a few,[12–15] do not include light extraction, which is essential for practical applications.

In this paper, we propose a concept of using an off-centered connecting output coupling waveguide for light extraction from a plasmonic nano-ring laser. The nano-ring laser is of particular interest because of the in-plane or radial lasing mode based on horizontal plasmonic confinement. It helps to miniaturize the device to the deep subwavelength scale, which is even smaller than the coaxial laser and the nano-patch laser.[10,11] It also facilitates planar integration of the nano-ring laser with other nanophotonic circuits for photonic-system-on-chip. To extract light from a circular cavity laser, evanescent field coupling through a bus waveguide in close proximity to a laser cavity is commonly used.[14] The setback of this approach is that it requires a stringent control and material filling for the gap between the waveguide and the cavity, as the coupling efficiency is highly sensitive to the gap distance and medium. As a unique and different approach from the evanescent coupling, our proposed scheme is based on a butt-jointed waveguide, which splits the plasmon mode for light extraction. The approach relaxes the stringent requirement on the coupling gap. As we will show later, it is revealed for the first time that the cavity mode rotates with the position of the butt-joint point, and subsequently, it affects the output coupling efficiency. Our numerical design shows that the coupling efficiency can be varied up to more than 50%.

Our propose structure is shown in Fig. 1. Our ultra-small plasmonic nanolaser is based on a metallic-semiconductor ring cavity. The laser comprises a submicron width semiconductor waveguide in ring configuration, covered with silver on both sides of the waveguide. The metallic-semiconductor waveguide enables light confinement well beyond the diffraction limit of light, which is hardly possible with any ordinary semiconductor or polymer waveguides. The loss incurred by the metal is compensated by the gain provided by the direct bandgap III–V

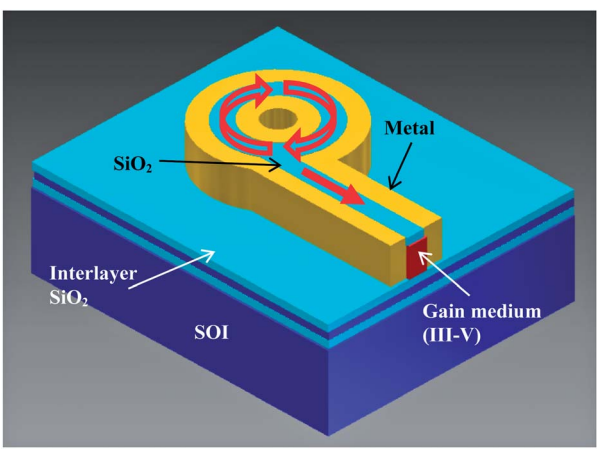

Fig. 1 Schematic of our proposed nano-ring laser with butt-joint outcoupling plasmonic waveguide (not drawn to scale). The top metal is removed in the figure to reveal the inner structure. The red-colored arrows suggest the possible light propagation direction.

*Data Storage Institute, A*STAR (Agency for Science, Technology and Research), Singapore. E-mail: lee_chee_wei@dsi.a-star.edu.sg*

semiconductor, which is also expected to provide the necessary gain for lasing. The gain material could be InGaAsP-based and an effective material bandgap around 1500 nm. In the example structure in Fig. 1, the nano-ring laser is bonded onto a silicon-on-insulator (SOI) substrate through a silicon dioxide interlayer, which potentially allows integration of electronic-photonic functionalities on a single chip in the future. The top and bottom oxide layers provide vertical mode confinement to the waveguide structure.

In our simulations, we utilize the commercially available FDTD Solutions from Lumerical Solutions, Inc. The optimizations of our proposed scheme consist of two parts: (i) the nano-ring structure, and (ii) the outcoupling efficiency after the introduction of a butt-joint outcoupling waveguide, but with more emphasis on the latter. The former is briefly mentioned for the sake of completeness, since extensive optimization on the nano-ring laser has been published before,[16] and the results are adapted into our model here. We utilize the design with two cavity resonance cycles, $m = 2$, in our simulation, since the case with $m = 1$ has already been presented in ref. 16. Our optimized nano-ring laser has an inner radius, R, of 70 nm, and a gain waveguide width, W, of 100 nm. The particular cavity has a Q-value of 103, and a resonance wavelength of 1488 nm.

Next, we introduce an output coupling plasmonic waveguide to the nano-ring. The butt-joint configuration is selected because it eliminates stringent control on the fabrication of the coupling gap, and also it is a unique feature that is possible only in plasmonic devices. The optimum width of the output waveguide is investigated, as well as the joint location on the ring. The coupling or extraction efficiency, η_c, is estimated by[12,13]

$$\eta_c = \frac{\frac{1}{Q_T} - \frac{1}{Q_o}}{\frac{1}{Q_T}} \quad (1)$$

where Q_o and Q_T correspond to the Q-values for the cavity without output coupling and with output coupling, respectively. These two Q-values can be obtained from our 2D-FDTD simulations. The Q-value serves as a good representation of the overall cavity loss. Q_T comprises three components: (i) intrinsic loss of the cavity, *i.e.* the loss with no output coupling waveguide, (ii) loss due to the mode perturbation after introduction of the coupling waveguide, and (iii) loss representing the outcoupling to the output plasmonic waveguide mode. Components (ii) and (iii) are not separable in our simulation of cavity Q-values, and thus, the coupling efficiency calculated represents only the maximum efficiency achievable. From eqn (1), to get a high coupling efficiency, the Q-value after the introduction of the coupling waveguide must be much smaller than the case without outcoupling. However, a lower Q-value will lead to a higher laser threshold, which is definitely not desirable. Hence, these two competing factors have to be considered in our optimization.

The maximum attainable coupling efficiencies for the various output waveguide widths, W_{out}, connected along the axis of the ring center, are shown in Fig. 2, together with their respectively steady state out-of-plane H-field profiles. The mode

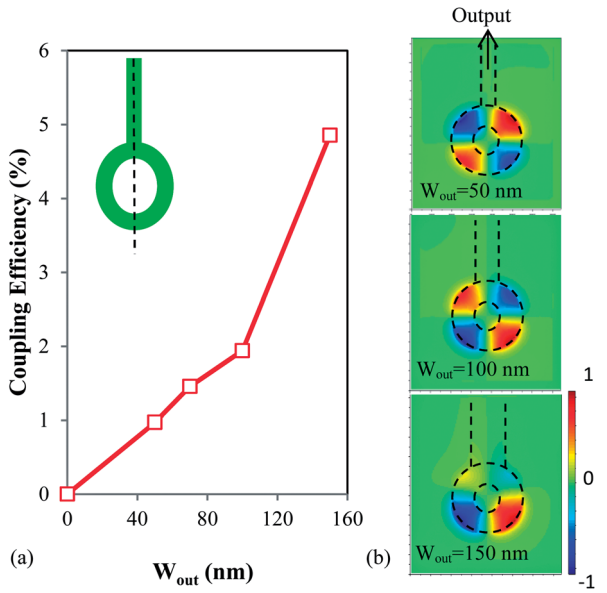

Fig. 2 (a) Coupling efficiencies for various output waveguide widths butt-jointed along the ring center axis, as shown in the inset, and (b) the H-field profiles for the output waveguide width = 50, 100 and 150 nm, where very minimal output light is seen.

profiles in Fig. 2(b) clearly show two resonance cycles ($m = 2$) inside the ring. From the figures, we can see that although the coupling efficiency increases with larger width, overall the efficiency is very low. We can observe from the steady-state mode profiles that, at the output junction, the field magnitude is always minimal. Such a mode profile will ensure that the cavity mode will suffer the least loss, but this in turn leads to the least outcoupling as well. Hence, to increase the output coupling, the cavity mode should not have a minimum magnitude at the output junction, *i.e.*, the symmetry of the cavity mode must be broken.

Our approach to increase the coupling efficiency is by offsetting the connecting junction away from the ring center, which serves as a means to break the mode symmetry. The coupling efficiencies at different offset distances from the center axis of the ring, d_x, are shown in Fig. 3(a). The calculated threshold material gains are plotted in the same figure. W_{out} of 100 nm is used because it is not too small for potential fabrication, and also not too large to degrade the Q-value that increases the laser threshold. The results show that as d_x increases, the coupling efficiency increases. The highest coupling efficiency occurred rather abruptly when $d_x = 120$ nm, where the output waveguide is flush with the outer edge of the ring. This is also evident from the steady state H-field plots in Fig. 3(b). Interestingly, we can clearly observe that the cavity mode rotates with the shifting of the output junction, in such a way that the zero field magnitude is always at the junction. This can be seen as the self-regulating effort of the cavity mode to minimize losses. At $d_x = 120$ nm, the cavity mode is unable to find a symmetric configuration with zero magnitude at the output junction. Consequently, the mode symmetry is broken and we are able to obtain maximum outcoupling, and the

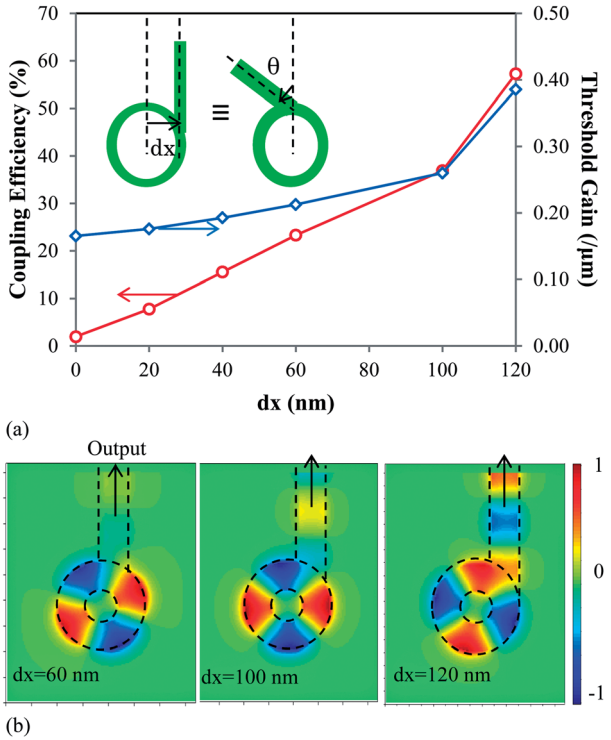

Fig. 3 (a) Coupling efficiencies at various butt-joint locations, and (b) the H-field profiles for $d_x = 60$, 100 and 120 nm. It can be seen that the cavity modes rotates as the butt-joint location changes.

output coupling increases drastically between $d_x = 100$ and 120 nm. This is an interesting phenomenon that has never been reported before. The off-centered shift can also be seen as rotating the waveguide around the center axis, as shown in the inset of Fig. 3(a), with $\sin\theta = d_x/(R + W/2)$, and hence, maximum outcoupling can be obtained when the output waveguide is parallel to the local mode propagation direction around the ring, or at $\theta = 90°$. The maximum coupling efficiency obtained is about 56%, with a material gain of 0.38 μm^{-1}, which is achievable using the InGaAsP-based material.[17] The material gain required increases with coupling efficiency, because it is equivalent to cavity loss. Further increase in d_x will shift the waveguide out of the ring and devastate the efficiency. Therefore, it is not of interest here. At $d_x = 120$ nm, a change of outcoupling waveguide width gives the same effect as the case of $d_x = 0$, where the maximum coupling efficiency is still achieved only at a W_{out} of 100 nm.

The outcoupling efficiency calculated by eqn (1) is verified with 3D FDTD simulation. The 3D output coupling is calculated by placing a transmission monitoring plane across the cross-section of the output waveguide to obtain the normalized transmission power. The two set of results show very close agreement and the maximum output efficiency obtained is about 52% obtained at $d_x = 120$ nm for the 3D simulation. The substrate leakage loss calculated from the 3D simulation is around 20% for all configurations.

After the design work, we proceeded on to the fabrication of the devices. The InGaAsP gain medium is commercially acquired and it is grown on an InP substrate by metal–organic

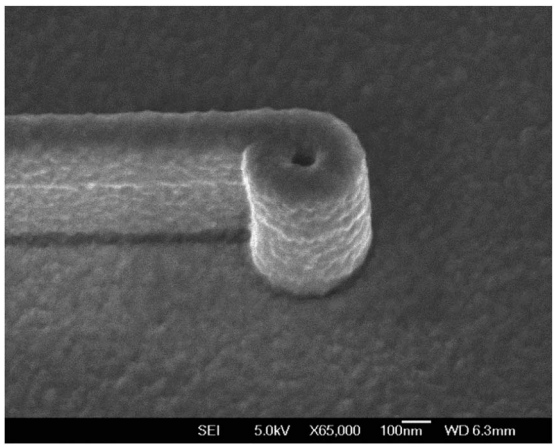

Fig. 4 Scanning electron micrograph of one of the fabricated structures. The nano-ring structure attached with an outcoupling waveguide is clearly visible, which demonstrates the feasibility of the design.

chemical vapor deposition (MOCVD). The active region is then bonded onto the Si substrate through interlayer bonding with thermal SiO_2,[18] followed by removal of the InP substrate in hydrochloric acid solution, leaving behind a submicron thin gain layer on the Si substrate. The submicron structures could be defined on the substrate *via* a hydrogen silsesquioxane (HSQ) resist with electron beam lithography, and then directly etched down with a chlorine recipe in an inductively coupled plasma reactive-ion-etching system (ICP-RIE) equipped with an elevated temperature stage at 250 °C. The process optimization is still in the preliminary stage; however, promising progress has been made. One of the scanning electron micrographs of the fabricated structure is shown in Fig. 4, where we can clearly see the nano-ring and the off-center outcoupling waveguide structures. The structure is covered by roughly 50 nm of silver on all sides deposited uniformly. Nevertheless, the initial fabricated structure shows that it is entirely possible to realize the designed submicron structure. In the determination of the coupling efficiency from an actual device, the method as described in ref. 19 is well-suited for the measurement of such a nanocavity. The method allows us to obtain the *Q*-value of the nanocavity, then, by using eqn (1) and comparing the *Q*-values of cavities with and without the outcoupling waveguide, we can calculate the coupling efficiency.

Conclusions

In summary, we have proposed a concept, with numerical verification, of an outcoupling scheme utilizing an offset butt-joint plasmonic waveguide for a nano-ring laser. The planar outcoupling is straightforward in terms of fabrication, and eliminates the tight control of the coupling gap in a conventional microring/disk-bus structure. The coupling efficiency obtained can be as high as 56% when the output waveguide is butt-jointed flush with the outer edge of the nano-ring. Similar outcoupling efficiencies are obtained both from calculation using eqn (1) and from 3D FDTD simulations, which verifies our

results. The efficient outcoupling comes with a trade-off of a higher material gain of 0.38 μm^{-1}. Nonetheless, the material gain is a reasonable value attainable by the III–V semiconductor. A promising initial result from the fabrication is also shown, where the nano-ring and outcoupling structure are clearly seen. This demonstrates the feasibility of the design.

The authors would like to express appreciation to Amy Liu from Lumerical Solutions, Inc. for guidance on simulation work with Lumerical FDTD Solutions, and Seng-Tiong Ho from Northwestern University for discussion. This work was supported by the Data Storage Institute of Science and Engineering Research Council of A*STAR (Agency for Science, Technology and Research), Singapore under grant no. DSI/13-100001.

Notes and references

1 O. Painter, R. K. Lee, A. Scherer, A. Yariv, J. D. O'Brien, P. D. Dapkus and I. Kim, Two-Dimensional Photonic Band-Gap Defect Mode Laser, *Science*, 1999, **284**, 1819–1821.

2 B. Ellis, M. A. Mayer, G. Shambat, T. Sarmieto, J. Harris, E. E. Haller and J. Vuckovic, Ultralow-threshold electrically pumped quantum dot photonic-crystal nanocavity laser, *Nat. Photonics*, 2011, **5**, 297–300.

3 J. Y. Suh, C. H. Kim, W. Zhou, M. D. Huntington, D. T. Co, M. R. Wasielewski and T. W. Odom, Plasmonic bowtie nanolaser arrays, *Nano Lett.*, 2012, **12**, 5769–5774.

4 M. T. Hill, Y.-S. Oei, B. Smalbrugge, Y. Zhu, T. D. Vries, P. J. V. Veldhoven, F. W. M. V. Otten, T. J. Eijkemans, J. P. Turkiewicz, H. D. Waardt, E. J. Geluk, S.-H. Kwon, Y.-H. Lee, R. N. Tzel and M. K. Smit, Lasing in metallic-coated nanocavities, *Nat. Photonics*, 2007, **1**, 589–594.

5 M. J. H. Marell, B. Smalbrugge, E. J. Geluk, P. J. Veldhoven, B. Barcones, B. Koopmans, R. Nötzel, M. K. Smit and M. T. Hill, Plasmonic distributed feedback lasers at telecommunications wavelengths, *Opt. Express*, 2011, **19**(16), 15109–15118.

6 M. P. Nezhad, A. Simic, O. Bondarenko, B. Slutsky, A. Mizrahi, L. Feng, V. Lomakin and Y. Fainmanet, Room-temperature subwavelength metallo-dielectric lasers, *Nat. Photonics*, 2010, **4**, 395–399.

7 K. Ding, M. T. Hill, Z. C. Liu, L. J. Yin, P. J. van Veldhoven and C. Z. Ning, Record performance of electrical injection subwavelength metallic-cavity semiconductor lasers at room temperature, *Opt. Express*, 2013, **21**, 4728–4733.

8 S.-H. Kwon, J.-H. Kang, C. Seassal, S.-K. Kim, P. Regreny, Y.-H. Lee, C. M. Lieber and H.-G. Park, Subwavelength plasmonic lasing from a semiconductor nanodisk with silver nanopan cavity, *Nano Lett.*, 2010, **10**, 3679–3683.

9 M. W. Kim and P.-C. Ku, Semiconductor nanoring lasers, *Appl. Phys. Lett.*, 2011, **98**, 201105.

10 K. Yu, A. Lakhani and M. C. Wu, Subwavelength metal-optic semiconductor nanopatch lasers, *Opt. Express*, 2010, **18**(9), 8790–8799.

11 M. Khajavikhan, A. Simic, M. Katz, J. H. Lee, B. Slutsky, A. Mizrahi, V. Lomakin and Y. Fainman, Thresholdless nanoscale coaxial lasers, *Nature*, 2012, **482**, 204–207.

12 K. Nozaki, H. Watanabe and T. Baba, Photonic crystal nanolaser monolithically integrated with passive waveguide for effective light extraction, *Appl. Phys. Lett.*, 2008, **92**, 021108.

13 Y. Halioua, A. Bazin, P. Monnier, T. J. Karle, G. Roelkens, I. Sagnes, R. Raj and F. Raineri, Hybrid III–V semiconductor/silicon nanolaser, *Opt. Express*, 2011, **19**, 9221–9231.

14 Q. Ding, A. Mizrahi, Y. Fainman and V. Lomakin, Dielectric shielded nanoscale patch laser resonators, *Opt. Lett.*, 2011, **36**, 1812–1814.

15 M. K. Kim, A. M. Lakhani and M. Wu, Efficient waveguide-couping of metal-clad nanolaser cavities, *Opt. Express*, 2011, **19**, 23504–23512.

16 C.-W. Lee, Q. Wang, G. Singh and S.-T. Ho, Design of ultra-small metallic-semiconductor nano-ring lasers, *IEEE Photonics Technol. Lett.*, 2013, **25**, 1153–1156.

17 L. A. Coldren and S. W. Corzine, Gain and current relations, in *Diode Lasers and Photonic Integrated Circuits*, John Wiley & Sons, Inc, New York, 1995, ch. 4, pp. 111–126.

18 Y. Wang, D. K. T. Ng, Q. Wang, J. Pu, C. Liu and S.-T. Ho, Low temperature direct bonding of InP and Si_3N_4-coated silicon wafers for photonic device integration, *J. Electrochem. Soc.*, 2012, **159**(5), H507–H510.

19 V. J. Sorger, R. F. Oulton, J. Yao, G. Bartal and X. Zhang, Plasmonic Fabry–Perot Nanocavity, *Nano Lett.*, 2009, **9**, 3489–3493.

